

# Comparison of Fixed and Fluidized Bed Reactors in the Steam Reforming of Raw Bio-oil with NiAl<sub>2</sub>O<sub>4</sub> Derived Catalyst

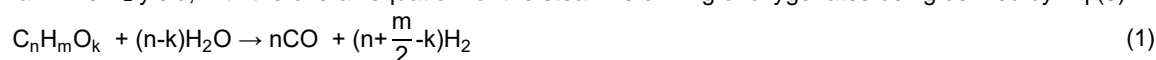
Leire Landa\*, Aingeru Remiro, Sergio Iglesias-Vazquez, José Valecillos, Ana G. Gayubo, Javier Bilbao

Department of Chemical Engineering University of the Basque Country (UPV/EHU), Bilbao 48080, Spain  
 leire.landa@ehu.eus

This work compares the performance of fixed and fluidized bed reactors in the SR of raw bio-oil with a NiAl<sub>2</sub>O<sub>4</sub> spinel derived catalyst, which has high activity and selectivity of H<sub>2</sub> in the raw bio-oil reforming. The SR runs have been carried out at 600 °C, steam/carbon molar ratio (S/C) of 3 and space time of 0.15 g<sub>catalyst</sub>/g<sub>bio-oil</sub>. The results of the fluidized bed reactor evidences lower initial bio-oil conversion and H<sub>2</sub> and CO<sub>2</sub> yields, due to the less effective gas-solid contact, however its stability is higher. The characterization of deactivated catalysts by Temperature Programed Reduction (TPR), X-Ray Diffraction (XRD), N<sub>2</sub> adsorption-desorption and Temperature Programed Oxidation (TPO) evidences that the main deactivation cause is coke deposition, that is noticeably higher in the fixed bed reactor (73 wt%) than in the fluidized bed (17 wt%). The TPO profiles for catalysts used in both reactors show two combustion domains, at low and high temperature. The reactor type does not affect the amount of coke that burns below 500 °C (coke I, amorphous), but notably affects both the amount and morphology of the coke burning at higher temperature (coke II, more graphitic). The use of fixed bed reactor leads to a noticeable higher formation of coke II, which contains heterogeneous carbon filaments and also carbon spheres, the latter not being formed in the fluidized bed. These differences in the amount and nature of the coke deposited explain the differences in stability of the catalyst in both reactors.

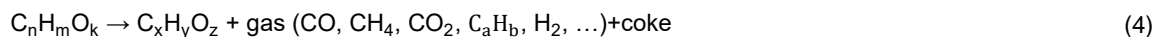
## 1. Introduction

With increasing global population, industrialization and urbanization, energy demand is rapidly rising. About 85 % of the current overall energy consumption worldwide is obtained from non-renewable resources (coal, natural gas, oil) (Abdalla et al., 2018). However, the depletion of fossil fuels, the implementation of stricter regulations and the social environmental awareness has attracted increasing attention on energy production from renewable sources, with hydrogen playing an important role as an energy vector in this crucial transition, because its use is free of toxic gas formation and CO<sub>2</sub> emissions (Lepage et al., 2021). Although hydrocarbons are currently the main feedstock used for H<sub>2</sub> production (mainly by steam reforming of natural gas), the need to increase the integration of technologies by means of processes that use renewable energy sources and do not contribute to CO<sub>2</sub> generation will become unavoidable in a near future (Nikolaidis and Poullikkas, 2017). Among different options, the steam reforming (SR) of bio-oil obtained from fast pyrolysis of lignocellulosic biomass is a promising and economically viable technology for H<sub>2</sub> production, which avoids the costly elimination of the water needed for other routes of bio-oil valorization, and is considered a CO<sub>2</sub> neutral process as the plants take the CO<sub>2</sub> for their growth. Likewise, negative CO<sub>2</sub> emissions can be achieved if the CO<sub>2</sub> produced in the reforming process is captured ex situ or in situ (Vicente et al., 2009). The overall reaction for the SR of oxygenates involves reforming reaction to produce (CO+H<sub>2</sub>) (Eq (1)) and the subsequent water-gas-shift (WGS) reaction (Eq (2)), to maximize H<sub>2</sub> yield, with the overall equation for the steam reforming of oxygenates being defined by Eq (3):





H<sub>2</sub> yield is also affected by reactions occurring in parallel to oxygenates reforming and WGS reactions, such as decomposition/cracking (Eq (4)), reforming of decomposition products (CH<sub>4</sub> and hydrocarbons, Eq (5) and Eq (6), respectively), and interconversion of oxygenates (Eq (7)). Moreover, coke formation (by hydrocarbons decomposition (Eq (8)) and Boudouard reaction (Eq (9))) and its gasification reaction (Eq (10)) should be considered, as they affect catalyst stability.



Ni-based catalysts are the most studied for SR of bio-oil (Gao et al., 2017; Bizkarra et al., 2018), but their rapid deactivation by coke deposition is a challenge to overcome for the industrial implementation of this process (Zhao et al., 2020). The stability of the catalysts is notably affected not only by the operating conditions (temperature, steam-to-carbon (S/C) molar ratio and space time), but also by the fluid dynamic regime in the reactor. The studies in fixed-bed evidence operating problems due to the rapid deactivation of the catalyst, and even gas flow blockage (Wang et al., 2007; Lan et al., 2010). The use of a fluidized bed reactor slightly attenuates these problems (Remon et al., 2013; Fu et al., 2014), which can be minimized by using a system with two steps in series, with the first one aimed at the controlled deposition of pyrolytic lignin (Valle et al., 2018). The objective of this work is to compare the performance of fixed and fluidized bed reactors in the SR of raw bio-oil with a NiAl<sub>2</sub>O<sub>4</sub> spinel derived catalyst, which has high activity and selectivity of H<sub>2</sub> in the raw bio-oil reforming and can be fully regenerated by combustion at 850 °C (Remiro et al., 2018). For that purpose, the evolution with reaction time of products yields has been analyzed, as well as the nature and amount of coke deposited, and structural and physical properties of the used catalysts, in order to explain the deactivation behavior in both reactors.

## 2. Experimental

### 2.1 Bio-oil

The raw bio-oil was supplied by BTG Bioliquids BV (The Netherlands) and synthesized from fast pyrolysis of pine sawdust in a conical rotatory reactor. Its physical-chemical properties are as follows: water content, determined by using Karl-Fischer titration (KF-Titrino Plus 870), 26 wt%; density, 1.105 g/ml; viscosity at 40 °C, 250 cP (Brookfield DV2T Ametek); pH, 2.5-3.5 and empirical formula C<sub>4.6</sub>H<sub>6.2</sub>O<sub>2.4</sub> (water-free basis), obtained by CHO analysis (Leco CHN-932 analyzer). The detailed raw bio-oil composition was determined with a Shimadzu QP2010S gas chromatography/mass spectrometer (GC/MS) provided with a BPX-5 column (50 m × 0.22 mm × 0.25 μm) and mass selective detector. The main compounds are ketones, acids, phenols (guaiacol), esters, saccharides (levoglucosan), aldehydes, furans/furanones, alcohols, and ethers.

### 2.2 Catalyst

The precursor NiAl<sub>2</sub>O<sub>4</sub> spinel (with 33 wt% Ni) was synthesized by the co-precipitation method (Arandia et al., 2020), mixing aqueous solutions of hexahydrated nickel nitrate (Ni(NO<sub>3</sub>)<sub>2</sub>·6H<sub>2</sub>O, Panreac, 99 %) and nonahydrated alumina nitrate (Al(NO<sub>3</sub>)<sub>3</sub>·9H<sub>2</sub>O, Panreac, 98 %) and adding dropwise a 0.6 M solution of ammonium hydroxide (NH<sub>4</sub>OH, Fluka, 5 M) as the precipitating agent, until reaching a pH of 8. The precipitate was recovered by filtration and washed with distilled water to remove the remaining ammonium ions. It was then dried for 12 h, calcined at 850 °C for 4 h with a heating ramp of 10 °C/min, and crushed and sieved to obtain particle sizes in the 150-250 μm range.

The physical properties of the fresh (reduced) and deactivated catalysts (BET surface area, pore volume and mean pore diameter), were characterized by adsorption-desorption of N<sub>2</sub> in a Micromeritics ASAP 2010. Temperature Programmed Reduction (TPR) analysis was carried out in a Micromeritics AutoChem II 2920 apparatus for determining the reducibility of the metal species. The structural properties of fresh (reduced) and used catalysts were analyzed by X-ray diffraction (XRD), measured on a Bruker D8 Advance diffractometer with a CuK $\alpha$ 1 radiation, in order to calculate the average Ni crystal size (using Scherrer equation) and the crystalline state of coke deposits. The amount and nature of coke deposited on used catalyst samples has been determined by Temperature Programmed Oxidation (TPO) in a TA-Instruments TGA-Q5000IR thermobalance, coupled in line with a mass spectrometer (Thermostar Balzers Instrument) for monitoring the CO<sub>2</sub> signal, that has been used for quantifying the coke content because the oxidation of Ni during combustion masks the thermogravimetric signal.

### 2.3 Reaction equipment, operating conditions and reaction indices

The kinetic runs have been performed in an automatized reaction equipment (MicroActivity-Reference, PID Eng & Tech) provided with two units in series for thermal treatment (Unit 1) and catalytic reforming (Unit 2) of bio-oil (Arandia et al., 2020). The Unit 1 is a U-shaped steel tube (inner diameter = 0.75 in) at 500 °C for vaporization of bio-oil and controlled deposition of pyrolytic lignin (PL) formed by re-polymerization of oxygenates (mainly phenolic compounds), in order to attenuate the subsequent deactivation of the SR catalyst in the reactor (Unit 2). The Unit 2 is a stainless steel tube (22 mm of internal diameter, total length of 460 mm and effective reaction length of 10 mm), which is operated with downwards (fixed bed) or upwards (fluidized bed) flux. The catalytic bed is located over a layer of quartz wool and consists of the catalyst mixed with inert solid (SiC, with particle size of 75  $\mu$ m), in order to improve the bed isothermicity (in fixed bed) and the fluid dynamics (in the fluidized bed). An injection pump (Harvard Apparatus 22) was used for feeding the bio-oil (0.06 ml/min) and a 307 Gilson pump for co-feeding the additional water required according to the desired steam to carbon (S/C) molar ratio. The reaction products were analyzed in a Micro GC Varian CP-490 connected in-line to the reactor through an insulated line (130 °C) to avoid condensation of the products, and equipped with three analytic channels: molecular sieve MS5 for quantifying H<sub>2</sub>, O<sub>2</sub>, N<sub>2</sub>, CH<sub>4</sub> and CO; PPQ column for light hydrocarbons (C<sub>2</sub>-C<sub>4</sub>), CO<sub>2</sub> and water; and Stabilwax for oxygenated compounds (C<sub>2</sub>+ ) and water. Prior to each reaction, the NiAl<sub>2</sub>O<sub>4</sub> spinel is reduced in situ under a H<sub>2</sub>-N<sub>2</sub> (10 vol% H<sub>2</sub>) at 850 °C for 4 h, thus obtaining the active Ni metallic phase well-dispersed on the support of alumina. The SR experiments were carried out at atmospheric pressure and 600 °C, with S/C of 3 and space time of 0.15 g<sub>catalyst</sub>h/g<sub>bio-oil</sub>. In both reactors inert gas (N<sub>2</sub>) was co-fed with the bio-oil and water, so that the linear gas velocity (u) at reaction conditions is 6 times the minimum fluidization velocity (u<sub>f,min</sub>) in the fluidized bed reactor.

The catalyst performance was quantified according to the carbon conversion to gas (Eq (11)), H<sub>2</sub> yield (Eq (12)) and yield of carbon products (CO<sub>2</sub>, CO, CH<sub>4</sub>, and HC) (Eq (13)):

$$X = \frac{F_{\text{out, gas}}}{F_{\text{in}}} \quad (11)$$

$$Y_{\text{H}_2} = \frac{F_{\text{H}_2}}{F_{\text{H}_2}^0} \quad (12)$$

$$Y_i = \frac{F_i}{F_{\text{in}}} \quad (13)$$

where F<sub>out, gas</sub> is the molar flow rate of the total carbon in gaseous product (CO<sub>2</sub>, CO, CH<sub>4</sub> and light hydrocarbons, in C equivalent units) at the reactor outlet; F<sub>in</sub> is the molar flow rate of oxygenates at the reactor inlet in C units contained; F<sub>H<sub>2</sub></sub> is the H<sub>2</sub> molar flow rate in the product stream; F<sub>H<sub>2</sub></sub><sup>0</sup> is the stoichiometric molar flow rate, which is calculated as (2n + m/2 - k)/n F<sub>in</sub>, according to the global stoichiometry for the bio-oil (C<sub>n</sub>H<sub>m</sub>O<sub>k</sub>) steam reforming (including the WGS reaction) (Eq (3)) and F<sub>i</sub> is the carbon-based molar flowrate of the i product (CO<sub>2</sub>, CO, CH<sub>4</sub> and HC) in the effluent (out) stream of the reactor.

## 3. Results

Figure 1 shows the evolution with time on stream (TOS) of carbon conversion to gas and product distribution obtained in fixed bed (graph a) and fluidized bed (graph b) reactors. The comparison of the results in both reactors evidences that the fixed bed attains higher initial conversion and H<sub>2</sub> and CO<sub>2</sub> yields, close to the thermodynamic equilibrium, which remain almost constant along 2h. Subsequently, they rapidly decrease due to catalyst deactivation for the reforming of oxygenates and of hydrocarbons (HC, formed by oxygenates decomposition, Eq (4)), whose yield increases after 2 h on stream. Nonetheless, CO and CH<sub>4</sub> remain almost constant with TOS, because they are intermediate compounds in the overall reaction scheme, and their forming - disappearing reactions are similarly affected by the deactivation of the catalyst. In the fluidized bed reactor

(Figure 1b) there is not an initial stable period, so that the carbon conversion to gas and the yields of H<sub>2</sub> and CO<sub>2</sub> decrease steadily from the beginning of the reaction, but more slowly than in the fixed bed reactor. As a result, similar values of conversion and yield of H<sub>2</sub> and CO<sub>2</sub> are achieved after 5 h on stream in both reactors, in spite of the lower initial values in the fluidized-bed. In this latter reactor, CO yield increases, CH<sub>4</sub> yield decrease and HC yield remains nearly null, which evidences that catalyst deactivation also affects the WGS (Eq (2)) and methanation (reverse Eq (5)) reactions, but not noticeably the reforming of HC.

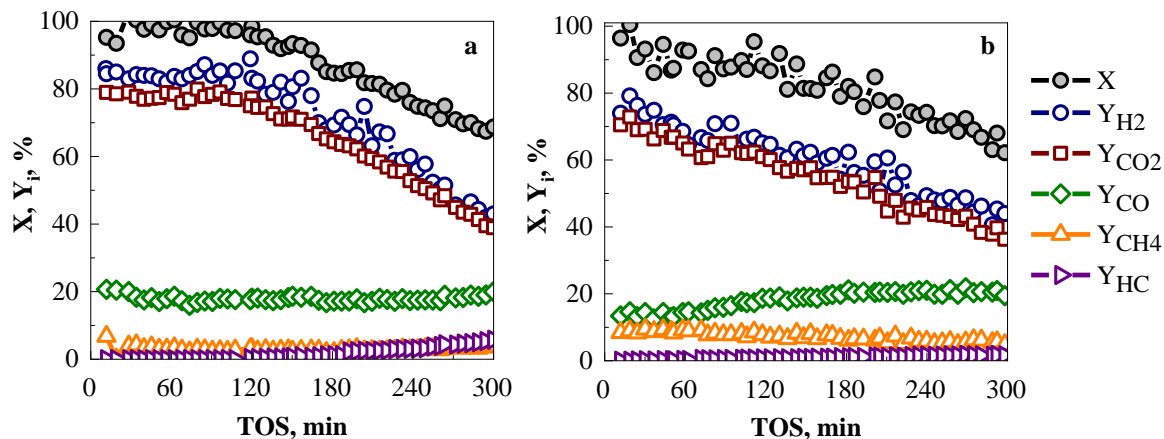


Figure 1: Evolution with time on stream (TOS) of carbon conversion and products yields in the SR of raw bio-oil in fixed (a) and fluidized (b) bed reactors, at 600 °C, S/C = 3, space time of 0.15 g<sub>catalyst</sub>/h/g<sub>bio-oil</sub>.

The less effective gas-solid contact taking place in the fluidized bed reactor explains the lower initial carbon conversion and H<sub>2</sub> and CO<sub>2</sub> yields (Remón et al., 2013). However, the catalyst deactivation rate is higher when the SR takes place in the fixed bed reactor. In order to explain the different stability in both reactors, the used catalyst have been characterized by several techniques to determine possible changes in Ni oxidation state and crystal size, in the porous structure, and the amount and characteristics of coke deposits.

Ni oxidation was ruled out as deactivation cause, as no significant reduction peaks were observed in the H<sub>2</sub>-TPR profiles of used catalyst (not shown), nor NiO species in their XRD diffractograms (Figure 2a). The absence of oxidized species is due to the highly reducing environment in the SR reaction, with a high H<sub>2</sub> content.

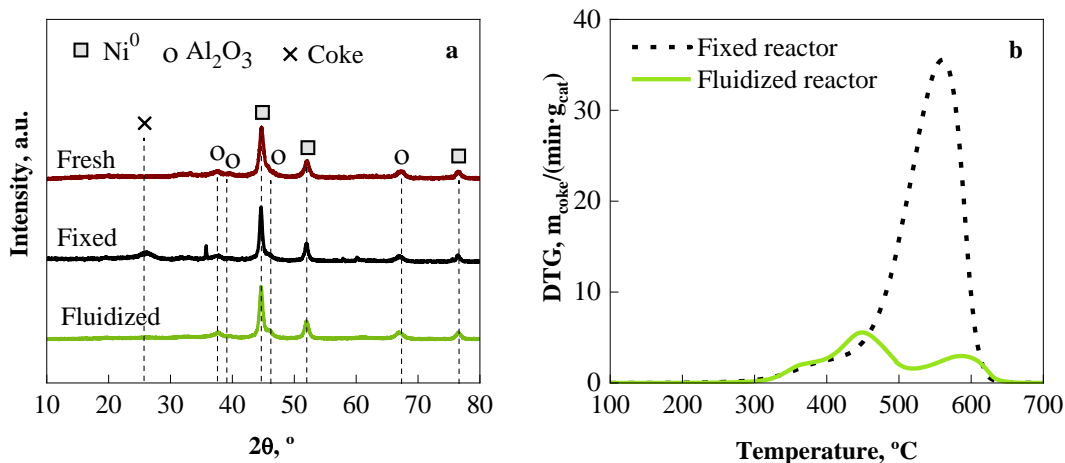


Figure 2. XRD diffractograms for fresh and used catalysts (a) and TPO profile for used catalysts (b)

The TPO profiles of used catalyst (Figure 2b) provide information on the total content of coke deposited (estimated from the total area under the TPO profiles) and on the nature and/or location of the coke in the structure of the catalyst (peak position). Both TPO profiles can be divided into two combustion domains, attributable to amorphous carbon (burning below 500 °C, coke I) and carbon filaments or graphitic coke (burning at high temperature, coke II) (He et al., 2020). Using a fixed bed reactor, the coke type II prevails, with maximum at 560 °C. However, the use of a fluidized system noticeably attenuates the formation of coke II, prevailing coke I formation. Consequently, the total coke amount is significantly higher in the fixed bed reactor (73 wt%) than in the fluidized bed (17 wt%). It is worth noting that the difference in the deactivation rate observed in both reactors

(Figure 1) is not as high as could be expected from the difference in the total coke amount deposited in both reactors, which evidences that, at the studied temperature, the coke type I (amorphous coke, with similar amount in both samples) has a more relevant role on the deactivation of the catalyst than the coke II.

The X-ray diffraction (XRD) analysis of the fresh-reduced and used catalysts provides information on the average size of Ni<sup>0</sup> crystals and the crystalline structure of coke deposits. On the one hand, the similar average size of Ni<sup>0</sup> crystals in Table 1 (obtained by Debye-Scherrer equation, at  $2\theta = 51.8^\circ$  (Ni<sup>0</sup> (200) plane)) for the fresh-reduced and used catalysts (15 nm and 17 nm, respectively) evidence almost insignificant Ni sintering in both reactors in the reaction conditions used. On the other hand, the presence of a broad peak at a diffraction angle  $2\theta = 26^\circ$  for the catalyst used in fixed bed suggests the presence of a high crystallinity coke (graphitic carbon), which is hardly observable for that used in fluidized bed.

The textural properties of fresh and deactivated catalyst samples (BET surface area, average pore diameter and pore volume) determined by means of N<sub>2</sub> adsorption-desorption are displayed in Table 1. The increase in BET surface area for the catalyst deactivated in fluidized bed reactor suggests a porous structure of the coke deposited, as that corresponding to filamentous carbon (coke II in the green curve of Figure 2a). Nevertheless, the BET surface area of the catalyst used in the fixed bed is the same as the fresh (reduced) catalyst, in spite of the high amount of coke II in this sample (black curve in Figure 2b) compared to that used in fluidized bed reactor. This result evidences a different morphology of coke II fraction for both deactivated samples.

Table 1: Physico-chemical properties of the catalysts fresh and used in fixed and fluidized bed reactors.

Catalyst	Reactor type	d <sub>Ni</sub> (nm)	S <sub>BET</sub> (m <sup>2</sup> /g)	V <sub>pore</sub> (cm <sup>3</sup> /g)	d <sub>pore</sub> (nm)
Fresh (reduced)	-	15	65.1	0.24	13.1
Deactivated	Fixed	17	64.2	0.17	12.9
	Fluidized	17	72.8	0.18	9.4

In order to ascertain the coke morphology, SEM images of the used catalysts are shown in Figure 3. The presence of thin, loose and short carbon filaments is observed in the sample used in fluidized bed (right image), with Ni particles on their tip. In the sample used in fixed bed (left image), carbon filaments are also observed, more heterogeneous than those formed in the fluidized bed, and, moreover, abundant carbon spheres are formed, which probably contribute to a partial clogging of the porous structure of the catalyst, and counteract the porosity created by the carbon filaments. The presence of carbon filaments is only observed in some particles of the sample used in the fluidized bed reactor, but most particles do not have carbon structures on their surface (as evidenced by SEM images with backscatter electron detector (BSD-SEM), not shown), which reveals that the coke is internally deposited in those particles (coke I). These results explain the more rapid deactivation in the fixed bed reactor (Figure 1a).

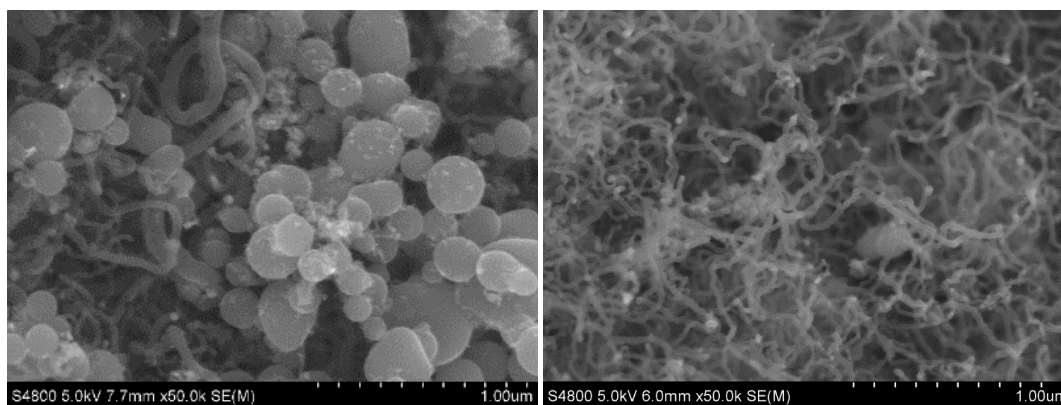


Figure 3: SEM images of the catalyst used in fixed bed (left) and fluidized bed (right).

#### 4. Conclusions

The fluid dynamic regime (fixed or fluidized bed) in the SR of bio-oil affects both the initial values of conversion and product yields and the amount and morphology of the coke deposited on NiAl<sub>2</sub>O<sub>4</sub> spinel derived catalyst, which in turn affects its stability. The less effective gas-catalyst contact in a fluidized bed reactor leads to lower initial carbon conversion and yields of H<sub>2</sub> and CO<sub>2</sub>, but slightly improves the catalyst stability due to a lower coke deposition (13 wt%) than in the fixed bed (73 wt%), and with different morphology. In both regimes the coke deposits are constituted by two fractions: amorphous fraction (with similar amount in both reactors)

and the main impact on deactivation, and structured and graphitic fraction (being the major fraction in the fixed bed reactor) with lower impact on deactivation composed of carbon filaments (in both reactors) and carbon spheres (only in the fixed bed reactor). The small difference in the stability of the fixed and fluidized bed reactors observed in this study is most probably due to the use of a prior thermal treatment unit, that avoids the risk of clogging of the reactor and improves the catalyst stability.

In conclusion, the original reaction system consisting of two units in series, with thermal treatment unit followed by a fluidized bed reactor, is got option for the industrial-scale implementation of bio-oil SR. Although the fixed bed avoids problems of attrition and fines entrainment, an overall superior performance could be envisioned for the fluidized reactor for its industrial-scale operation, because it ensures better control of the process variables and higher catalyst stability, provided that a good fluid dynamics is attained (with not excessive  $u/u_{f,\min}$  ratio) to provide good gas-solid contact.

### Acknowledgments

This work has been carried out with the financial support of the grant RTI2018-100771-B-I00 funded by MCIN/AEI/10.13039/501100011033 and by "ERDF A way of making Europe", the European Commission (HORIZON H2020-MSCA RISE 2018. Contract No. 823745) and the Department of Education, Universities and Investigation of Basque Government (Project IT1218- 19 and PhD grant PRE\_2021\_2\_0147 for L. Landa).

### References

- Abdalla A.M., Hossain S., Nisfindy O.B., Azad A.T., Dawood M., Azad A.K., 2018, Hydrogen production, storage, transportation and key challenges with applications: A review, *Energy Conversion and Management*. Elsevier Ltd, 165, 602–627.
- Arandia, A., Remiro, A., Valle, B., Bilbao, J., Gayubo, A. G., 2020, Deactivation of Ni spinel derived catalyst during the oxidative steam reforming of raw bio-oil. *Fuel*, 276, 117995.
- Bizkarra, K., Bermudez, J. M., Arcelus-Arillaga, P., Barrio, V. L., Cambra, J. F., Millan, M., 2018, Nickel based monometallic and bimetallic catalysts for synthetic and real bio-oil steam reforming, *International Journal of Hydrogen Energy*, 43(26), 11706–11718.
- Fu, P., Yi, W., Li, Z., Bai, X., Zhang, A., Li, Y., Li, Z., 2014, Investigation on hydrogen production by catalytic steam reforming of maize stalk fast pyrolysis bio-oil. *International Journal of Hydrogen Energy*, 39(26), 13962–13971.
- Gao, N., Han, Y., Quan, C., Wu, C., 2017, Promoting hydrogen-rich syngas production from catalytic reforming of biomass pyrolysis oil on nanosized nickel-ceramic catalysts, *Applied Thermal Engineering*, 125, 297–305.
- He, L., Liao, G., Hu, S., Jiang, L., Han, H., Li, H., Ren, Q., Mostafa, M. E., Hu, X., Wang, Y., Su, S., Xiang, J., 2020, Effect of temperature on multiple competitive processes for co-production of carbon nanotubes and hydrogen during catalytic reforming of toluene, *Fuel*, 264.
- Lan, P., Xu, Q., Zhou, M., Lan, L., Zhang, S., Yan, Y., 2010, Catalytic Steam Reforming of Fast Pyrolysis Bio-Oil in Fixed Bed and Fluidized Bed Reactors. *Chemical Engineering & Technology*, 33(12), 2021–2028.
- Lepage, T., Kammoun, M., Schmetz, Q., Richel, A., 2021, Biomass-to-hydrogen: A review of main routes production, processes evaluation and techno-economical assessment, *Biomass and Bioenergy*, 144, 105920.
- Nikolaïdis, P., Poullikkas, A., 2017, A comparative overview of hydrogen production processes, *Renewable and Sustainable Energy Reviews*, 67, 597–611.
- Remiro, A., Arandia, A., Oar-Arteta, L., Bilbao, J., Gayubo, A. G., 2018, Regeneration of NiAl<sub>2</sub>O<sub>4</sub> spinel type catalysts used in the reforming of raw bio-oil, *Applied Catalysis B: Environmental*, 237, 353–365.
- Remón, J., Broust, F., Volle, G., García, L., Arauzo, J., 2015, Hydrogen production from pine and poplar bio-oils by catalytic steam reforming. Influence of the bio-oil composition on the process, *International Journal of Hydrogen Energy*, 40(16), 5593–5608.
- Remón, J., Medrano, J. A., Bimbela, F., García, L., Arauzo, J., 2013, Ni/Al-Mg-O solids modified with Co or Cu for the catalytic steam reforming of bio-oil, *Applied Catalysis B: Environmental*, 132–133, 433–444.
- Valle, B., Aramburu, B., Benito, P. L., Bilbao, J., Gayubo, A. G., 2018, Biomass to hydrogen-rich gas via steam reforming of raw bio-oil over Ni/La<sub>2</sub>O<sub>3</sub>- $\alpha$ -Al<sub>2</sub>O<sub>3</sub> catalyst: Effect of space-time and steam-to-carbon ratio, *Fuel*, 216.
- Vicente, J., Remiro, A., Atutxa, A., Ereña, J., Gayubo, A.G., Bilbao, J., 2009, In situ capture of CO<sub>2</sub> during steam reforming of ethanol over Ni/SiO<sub>2</sub> catalyst for hydrogen production, *Chemical Engineering Transactions*, 17, 1567-1572.
- Wang, Z., Pan, Y., Dong, T., Zhu, X., Kan, T., Yuan, L., Torimoto, Y., Sadakata, M., Li, Q., 2007, Production of hydrogen from catalytic steam reforming of bio-oil using C<sub>12</sub>A<sub>7</sub>-O<sup>-</sup>-based catalysts, *Applied Catalysis A: General*, 320, 24–34.
- Zhao, Z., Situmorang, Y. A., An, P., Chaihad, N., Wang, J., Hao, X., Xu, G., Abudula, A., Guan, G., 2020, Hydrogen Production from Catalytic Steam Reforming of Bio-Oils: A Critical Review, *Chemical Engineering & Technology*, 43(4), 625–640.